ELSEVIER

Ceramics International 31 (2005) 241–247

CERAMICS INTERNATIONAL

www.elsevier.com/locate/ceramint

Synthesis of $Li_{1-x}Ni_{1+x}O_2$ using malonic acid as a chelating agent

Titipun Thongtem*, Somchai Thongtem

Faculty of Science, Chiang Mai University, Chiang Mai 50200, Thailand

Received 16 February 2004; received in revised form 12 March 2004; accepted 3 May 2004
Available online 21 August 2004

Abstract

$Li_{1-x}Ni_{1+x}O_2$ powder was synthesized by polymerised complex method using malonic acid as a chelating agent. The carboxylate precursor was calcined in the temperature range 650–800 °C for 14–48 h. The TG curves of malonic acid, lithium acetate dihydrate, nickel acetate tetrahydrate and the precursor were studied at 29.52–600 °C. The FTIR spectra of the precursor without and with 650–800 °C calcination were used to explain the vibrational bonding. At 750 °C and above, only $Li_{1-x}Ni_{1+x}O_2$ phase was detected. The maximum $[I_{(003)}/I_{(104)}]$ and minimum $[I_{(006+102)}/I_{(101)}]$ intensity ratios of the XRD spectra were used to determine the optimum temperature and time of calcination for preparation of $Li_{1-x}Ni_{1+x}O_2$ powder. In addition, formation mechanism of $Li_{1-x}Ni_{1+x}O_2$ is proposed. The content of nickel, lithium, $Ni^{3+}/(Ni^{3+} + Ni^{2+})$ and mean oxidation state of nickel at 650–800 °C were determined and they show very good agreement. The SEM micrograph is also used to explain the morphology of the powder.

Keywords: $Li_{1-x}Ni_{1+x}O_2$; Malonic acid; Polymerised complex method

1. Introduction

Current lithium–nickel–oxygen batteries have been shown to be nonstoichiometric but are very useful as rechargeable devices. The stoichiometric compound $LiNiO_2$ would be expected to have more ideal properties, yet its synthesis has remained elusive. As a layered transition metal oxide, $LiNiO_2$ would have the nickel ion surrounded by six oxygen ions to form the $LiNiO_2$ infinite slabs by edge-sharing of the NiO_2 layers in octahedral sites [1]. The ideal layer of $LiNiO_2$ would have an array of close packed oxygen with slight distortion and rhombohedral structure with the $R\bar{3}m$ space group [1,2]. It would be expected to show high discharge capacity and good reversibility [3–5].

Nonstoichiometric $LiNiO_2$, with a relative excess of Ni over Li, shows rather poor electrochemical performance due to nickel ions residing in the lithium ion sites [6–8]. $Li_{1-x}Ni_{1+x}O_2$ can be prepared by solid-state [9–11] and chemical solution methods [12–14]. There are several disadvantages for the solid-state method such as irregular morphology and broader particle size distribution.

Chemical solution systems have been shown to offer improved solid-state structures and novel products for such compounds as $LiNiO_2$ [1,15,16], $LiMn_2O_4$ [17,18], and $LiCoO_2$ [19], probably due to the ability of the dried precursors to give smaller particle size and more homogenous mixing prior to calcination. Dicarboxylic acids are used as chelating agents to keep the metal ions in solution, surrounded by oxygen ions, and oriented in such a way as to facilitate eventually solid oxide formation with good homogeneity upon calcination. The purpose of the research described here is to synthesize $Li_{1-x}Ni_{1+x}O_2$ by the polymerised complex method using malonic acid as a chelating agent and to find the optimum conditions (temperature and time) of calcination for preparation of $Li_{1-x}Ni_{1+x}O_2$ powder. The optimum condition was determined in order to obtain the product with good crystalline and high Ni^{3+} content leading to the best electrochemical performance.

* Corresponding author.
E-mail address: ttpthongtem@yahoo.com, ttpthongtem@hotmail.com (T. Thongtem).

0272-8842/$30.00
doi:10.1016/j.ceramint.2004.05.007

2. Experimental methods

The preparation of $Li_{1-x}Ni_{1+x}O_2$ powder from lithium acetate dihydrate and nickel acetate tetrahydrate through the carboxylate precursor is schematically shown in Fig. 1. Lithium acetate and nickel acetate were dissolved in ethanol to which the respective ion was 1:1 mole ratio. Malonic acid was used as a chelating agent. Following similar preparation procedures for the lithium manganese oxide [17], the malonic acid in ethanol was added such that the acid to total metal mole ratio was 1:1. The chelated ions were polymerised into gel with the acetates. The precursor was dried at 50–60 °C, precalcined at 450 °C for 6 h and further calcined at 650–800 °C for 14–48 h in air. The powder was finally obtained.

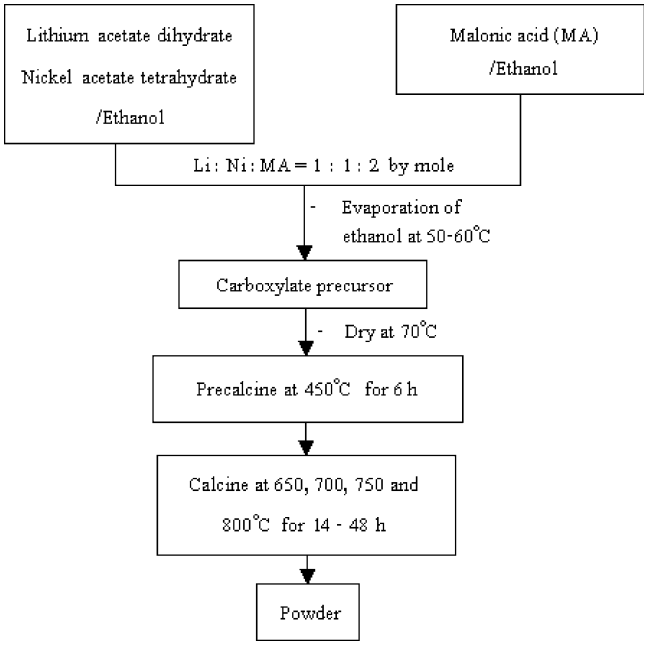

Fig. 1. Flow chart for preparation of $Li_{1-x}Ni_{1+x}O_2$ powder using malonic acid as a chelating agent.

The effect of temperature on the carboxylate precursor was characterized using thermogravimetric analyser (TGA) and Fourier transform infrared spectrometer (FTIR). The phase purity of the powder was analysed using an X-ray diffractometer (XRD) with Cu Kα as the target. The external morphology was observed using a scanning electron microscope (SEM). The total content of nickel and lithium were determined using an atomic absorption spectrophotometer (AAS). The content of Ni^{3+} was determined using a titration. The Ni^{3+} was reduced to Ni^{2+} by the excess ammonium iron(II) sulphate and back titration with the standard potassium permanganate solution. Then, $Ni^{3+}/(Ni^{3+} + Ni^{2+})$ of $Li_{1-x}Ni_{1+x}O_2$ and mean oxidation state of nickel were calculated.

3. Results and discussion

3.1. Thermal analysis

The TGA of malonic acid, lithium acetate dihydrate, nickel acetate tetrahydrate and the carboxylate precursor was studied in nitrogen atmosphere and are shown in Fig. 2.

The TG spectrum of malonic acid shows weight loss over the range of 170–280 °C. Weight loss of lithium acetate dihydrate was the result of the evaporation of adsorbed and lattice water and the decomposition of acetate ions at

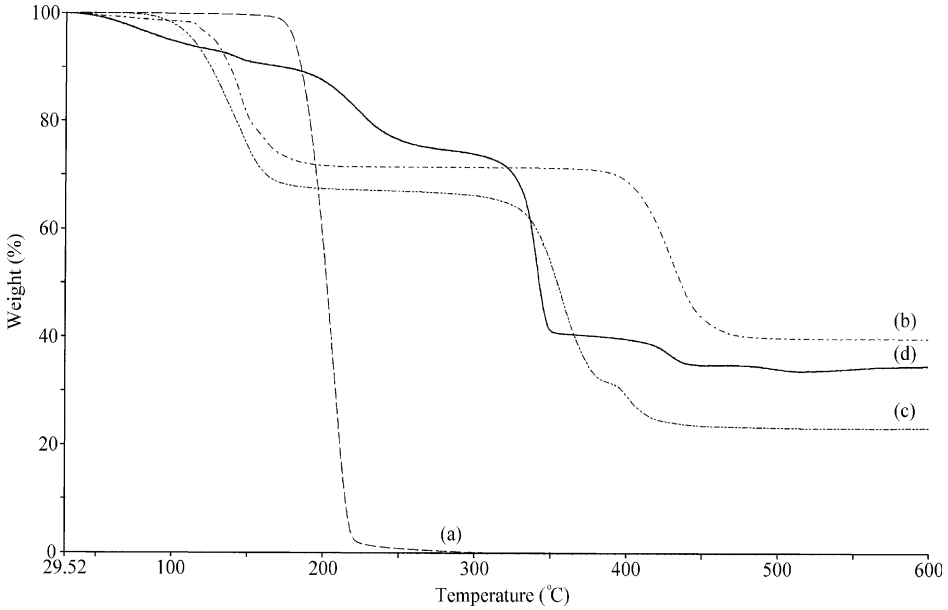

Fig. 2. TG spectra of (a) malonic acid, (b) lithium acetate dihydrate, (c) nickel acetate tetrahydrate and (d) the carboxylate precursor without calcination.

50–228 and 338–470 °C [1], respectively. The TG spectrum of nickel acetate tetrahydrate shows three discrete weight losses. They are the evaporation of the adsorbed and lattice water, the decomposition of acetate ions and the residual organic constituents at 56–209 [1], 271–390 [1] and 390–500 °C, respectively. But for the carboxylate precursor, it shows the weight loss of four steps resulting from the evaporation of ethanol and adsorbed water at 49–160 °C, the decomposition of malonic acid at 173–278 °C, the decomposition of acetate ions from the pyrolysis of lithium and nickel acetates at 287–363 °C and other organic compounds at 391–510 °C. It is likely that malonic acid can play the role on the decomposition of the acetate ions. Then, the weight loss is terminated showing that lithium nickel oxides are likely to form at 510 °C and above.

3.2. Vibrational spectra

The FTIR spectra of the carboxylate precursor without and with 650–800 °C calcination in air for 24 h are shown in Fig. 3. The spectrum for the precursor without calcination shows the broad band of O–H stretching of residual water and carboxylic acid over the range of 2500–3700 cm^{-1}. The asymmetric and symmetric COO stretching bands of the carboxylate group linked with metal ions are in the range of 1540–1620 and 1360–1450 cm^{-1}, respectively. Over the range of 1670–1700 cm^{-1}, the C–O stretching band was detected. It is likely to be from the residual carboxylic acids that are not involved in the coordination [20].

The spectra of the precursor with 650–800 °C calcination show a severe reduction in the intensity of the O–H stretching band. No carbonyl and carboxyl groups of organic compounds were detected at 650–800 °C. New peaks of the stretching and bending bands of CO_3^{2-} were detected at 1410–1510 and 850–870 cm^{-1}, respectively. The concentration of CO_3^{2-} is decreased with an increase in the calcination temperature. Very small concentration of CO_3^{2-} was detected at 800 °C. Peaks of the metal–oxygen were clearly detected at the vicinity of 550 cm^{-1}.

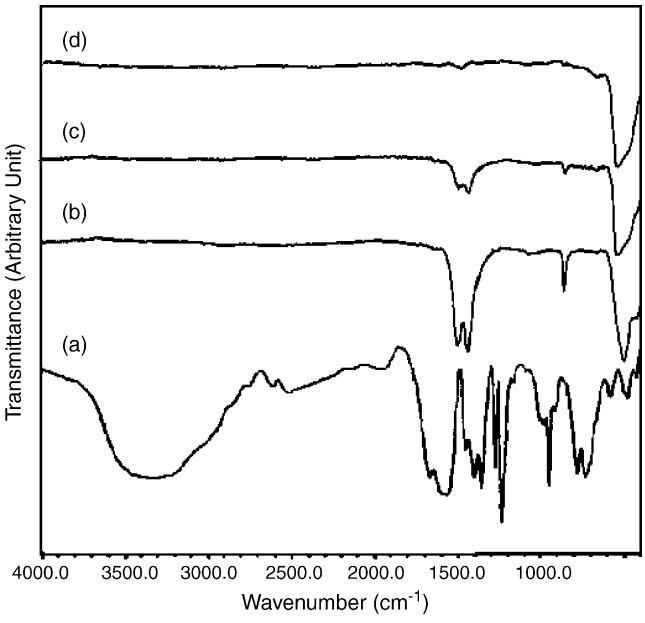

Fig. 3. FTIR spectra of the carboxylate precursor: (a) without calcination; (b–d) with 650, 750 and 800 °C calcination, respectively.

3.3. Phase analysis

The powder obtained from the carboxylate precursor with 650–800 °C calcination in air for 24 h was analysed using the XRD. The results are shown in Fig. 4. At 650 °C, the XRD peaks are broad showing a low degree of crystallinity with very fine grains. As the temperature was increased, the powder became more crystalline with larger grain size. The powder with 650 and 700 °C calcination is $Li_{1-x}Ni_{1+x}O_2$ ($0 \leq x < 1$) [21–23] containing $Li_2Ni_8O_{10}$ [24] and Li_2CO_3 [15] as impurities. The XRD peaks of either nonstoichiometric or stoichiometric phase diffracted from the same planes are at the same 2θ. Only the intensities are different [21–24]. At 750 and 800 °C, only $Li_{1-x}Ni_{1+x}O_2$ was detected.

3.4. Ordering of ions

The optimum temperature and time for preparation of lithium nickel oxide is identified by the maximum [$I_{(003)}/I_{(104)}$] and minimum [$I_{(006+102)}/I_{(101)}$] intensity ratios of the XRD spectra. At the optimum temperature and time, lithium, and nickel ions are at the most hexagonal ordering and least cation mixing [1,2,25,26], which is the key factor to promote the electrochemical performance of the oxide. The relation between the intensity ratios and the calcination temperature are shown in Fig. 5. The maximum and minimum intensity ratios obtained from the precursor with 650–800 °C calcination in air for 24 h are at 700 and 750 °C, respectively. Therefore, the best temperature is in the range of 700–750 °C. In the thermodynamic point of view, the entropy of mixing of the ions is the smallest [27]. Cations residing in their normal lattice sites will promote the diffusion of charge carriers resulting to good electrochemical performance such as the rechargeable capacity and reversibility [25]. Due to the minimum impurities, the temperature of 750 °C was selected.

3.5. Proposed mechanism

A possible mechanism for the formation of the different nonstoichiometric oxides would include the following details. During the calcination, the carboxylate precursor formed from the partial dehydration process would produce one nonstoichiometric and two stoichiometric phases. $Li_2Ni_8O_{10}(s)$ reacts with $Li_2CO_3(s)$ to form $Li_{1-x}Ni_{1+x}O_2(s)$ and Ni^{2+} is oxidised to Ni^{3+}. The possible

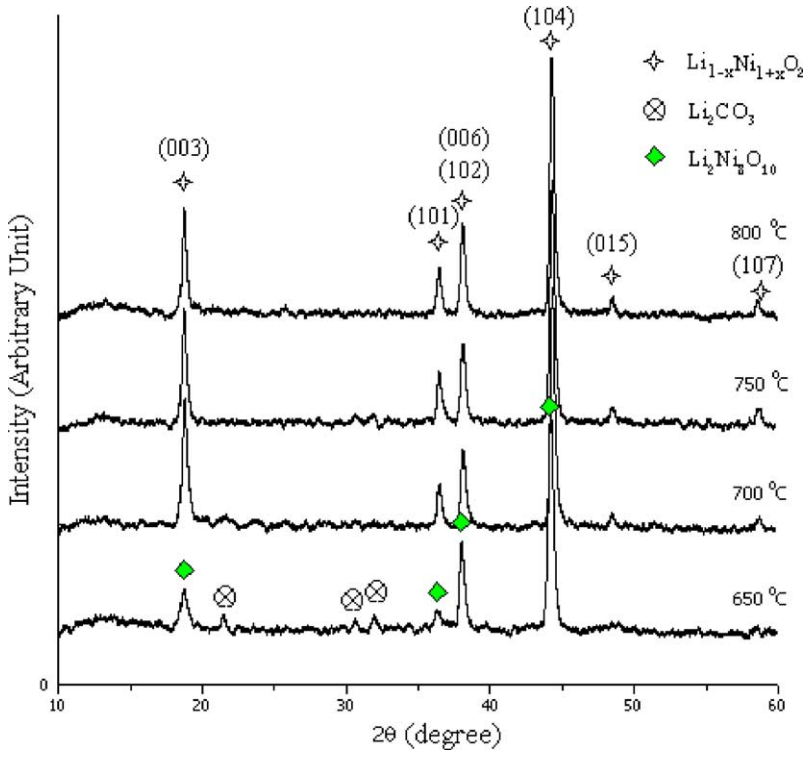

Fig. 4. XRD spectra of the carboxylate precursor with 650–800 °C calcination in air for 24 h.

reactions are likely to be the following:

Carboxylate precursor

$$\rightarrow Li_{1-x}Ni_{1+x}O_2(s) + Li_2Ni_8O_{10}(s) + Li_2CO_3(s) \quad (1)$$

$$(2+2x)Li_2Ni_8O_{10}(s) + (8x-4)Li_2CO_3(s) \rightarrow 16Li_{1-x}Ni_{1+x}O_2(s) + (18x-10)Li_2O(g) + (8x-4)CO_2(g) + (5x-3)O_2(g) \quad (2)$$

However, stoichiometric $LiNiO_2(s)$ can form at low calcination temperature. Impurities, degree of crystallinity and others are the parameters to play a role on the electrochemical performance as well. As the temperature is increased, lithium ions evaporate as lithium oxide [26,28] and diffuse into the surrounding atmosphere. The reaction is likely to be

$$(2+2x)LiNiO_2(s) \rightarrow 2Li_{1-x}Ni_{1+x}O_2(s) + 2xLi_2O(g) + xO_2(g) \quad (3)$$

The rate of lithium evaporation is increased with an increase in the calcination temperature. Vacancies form on lithium

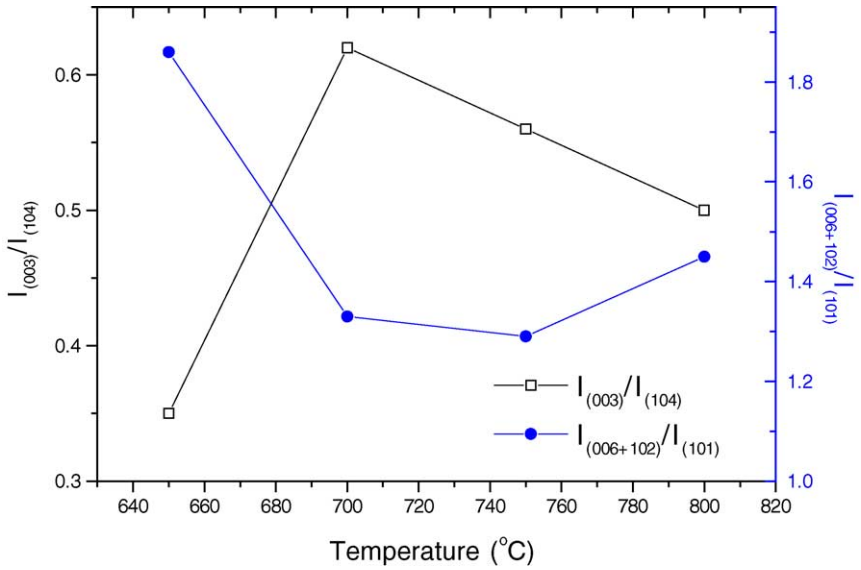

Fig. 5. Intensity ratios of $Li_{1-x}Ni_{1+x}O_2$ prepared from the carboxylate precursor with 650–800 °C calcination in air for 24 h.

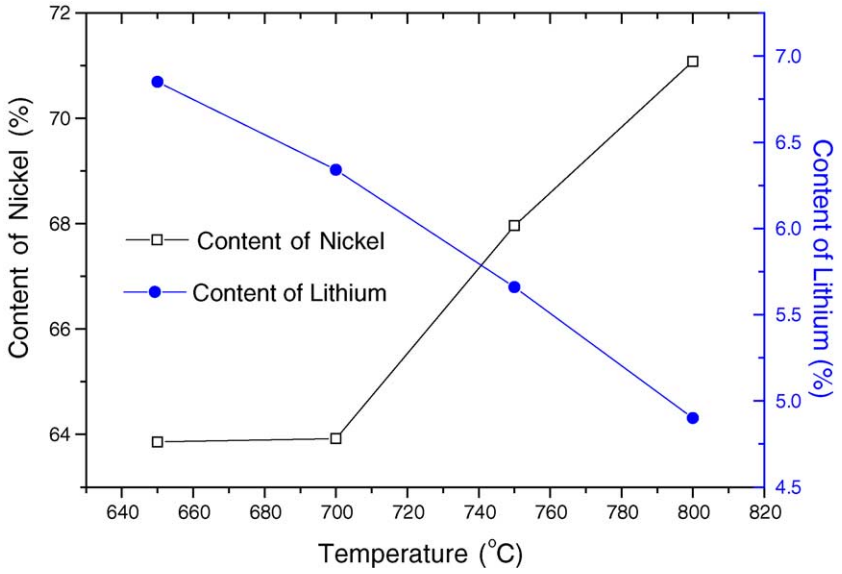

Fig. 6. Contents of nickel and lithium in $Li_{1-x}Ni_{1+x}O_2$ powder prepared from the carboxylate precursor with 650–800 °C calcination in air for 24 h.

lattice sites. The negative and positive charges of the whole lithium nickel oxide crystal are unbalanced. To maintain the electrical neutrality, Ni^{3+} ions are reduced to Ni^{2+} ions. The crystal structure of lithium nickel oxide is a cubic close packing of oxygen ions and the octahedral sites are filled in the alternative sequence of the nickel and lithium ions [25,29]. The ionic radii of Ni^{3+}, Ni^{2+} and Li^+ are 0.056, 0.069 and 0.076 nm, respectively [30,31]. Due to the electrical charge and size of ions, Ni^{2+} ions diffuse to reside in lithium ion vacancies [26]. The excess nickel ions form in the crystal. Therefore, the chemical formula is written as $Li_{1-x}Ni_{1+x}O_2$ [28]. The value of x is a parameter to identify whether the crystal is the rock salt or hexagonal structure [21].

3.6. Mean oxidation state of nickel

The contents of nickel, lithium and $Ni^{3+}/(Ni^{3+} + Ni^{2+})$ of $Li_{1-x}Ni_{1+x}O_2$ powder with 650–800 °C calcination in air for 24 h are shown in Figs. 6 and 7. At 650–800 °C, there were the existence of both Ni^{2+} and Ni^{3+}. The content of nickel was increased with an increase in the calcination temperature due to the evaporation of $Li_2O(g)$ resulting in the decreasing of the content of lithium. But for Ni^{3+} in the total nickel, it was increased to the maximum value at 750 °C due to the oxidation of Ni^{2+} in $Li_2Ni_8O_{10}(s)$ to Ni^{3+} as previously explained. The reduction process was established as well but the oxidation process was dominant.

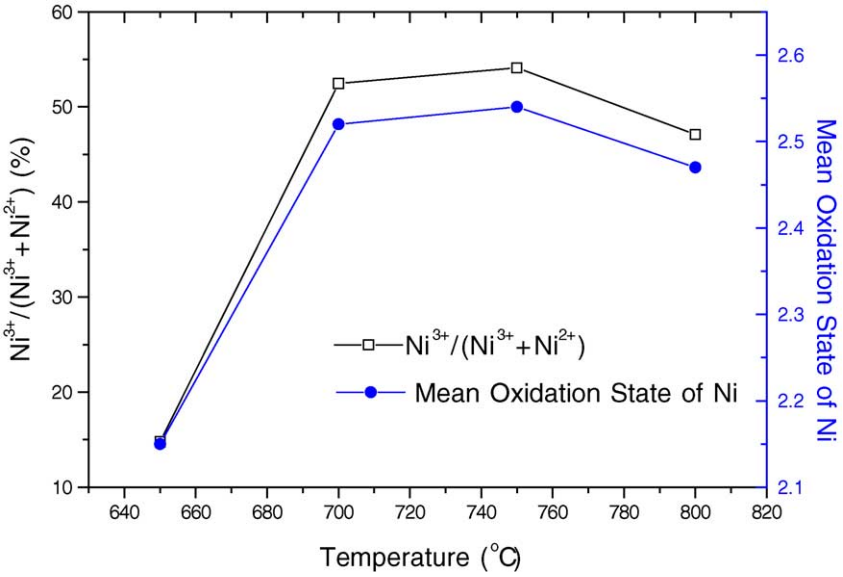

Fig. 7. Content of $Ni^{3+}/(Ni^{3+} + Ni^{2+})$ and mean oxidation state of nickel in $Li_{1-x}Ni_{1+x}O_2$ powder prepared from the carboxylate precursor with 650–800 °C calcination in air for 24 h.

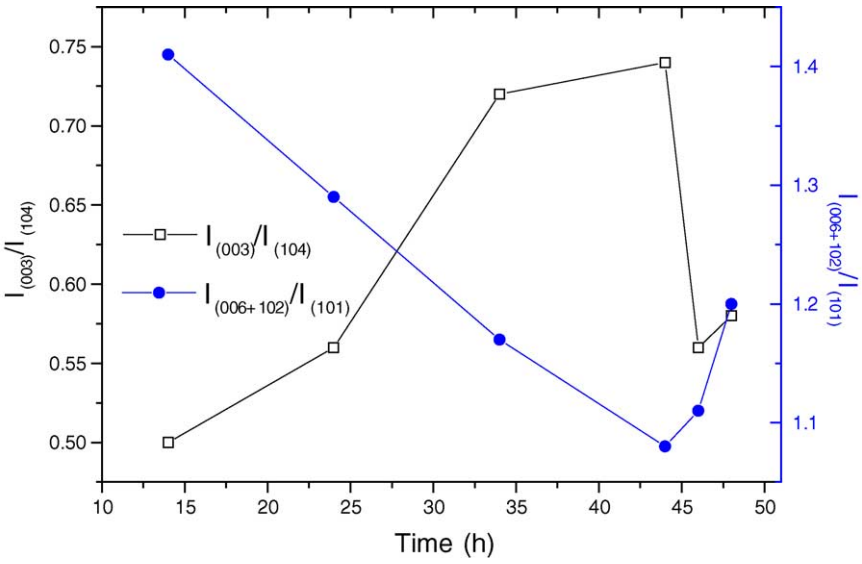

Fig. 8. Intensity ratios of $Li_{1-x}Ni_{1+x}O_2$ prepared from the carboxylate precursor with 750 °C calcination in air for 14–48 h.

At 800 °C, Li^+ evaporated very rapidly with the reduction of Ni^{3+} to Ni^{2+} in nonstoichiometric lithium nickel oxide by the reaction

$$(2+2y)Li_{1-x}Ni_{1+x}O_2(s) \rightarrow (2+2x)Li_{1-y}Ni_{1+y}O_2(s) + (2y-2x)Li_2O(g) + (y-x)O_2(g) \quad (4)$$

where y is more than x. Then, the content of Ni^{3+} was rapidly decreased.

Mean oxidation state of nickel in $Li_{1-x}Ni_{1+x}O_2$ was calculated using the equation

$$\text{Mean oxidation state} = 2 + N \quad (5)$$

where N is the mole fraction of Ni^{3+} in the total mole of nickel. Mean oxidation state of nickel in the powder prepared from the precursor with 650–800 °C calcination in air for 24 h is shown in Fig. 7. It is the maximum at 750 °C. This shows the correspondence of mean oxidation state of nickel, the maximum content of $Ni^{3+}/(Ni^{3+} + Ni^{2+})$ and the minimum intensity ratio.

3.7. Optimum calcination temperature and time

When the 750 °C calcination was kept constant and the time was varied between 14 and 48 h, the maximum and minimum intensity ratios are shown in Fig. 8. The optimum time for the calcination of the precursor is 44 h. At the

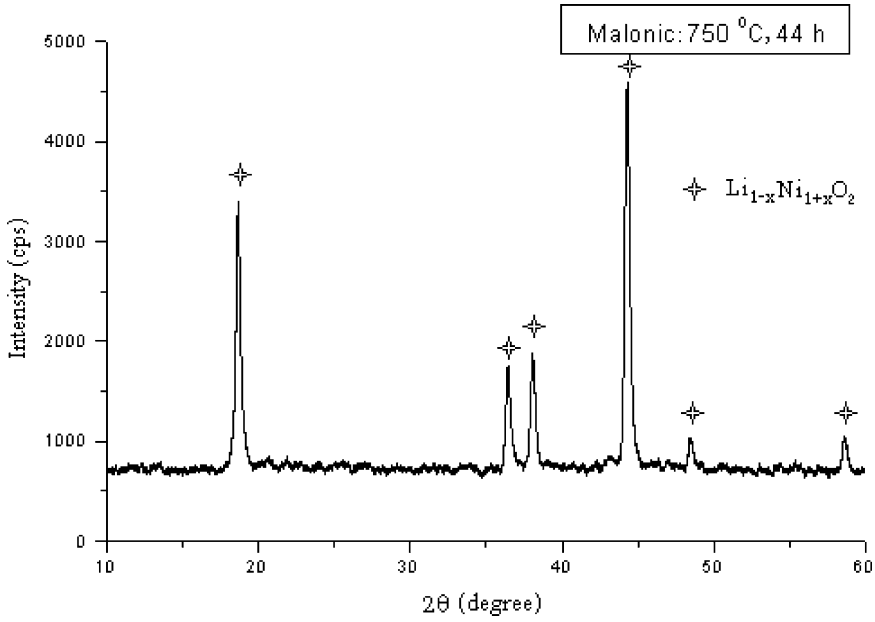

Fig. 9. XRD spectra of the carboxylate precursor calcined at the optimum temperature and time.

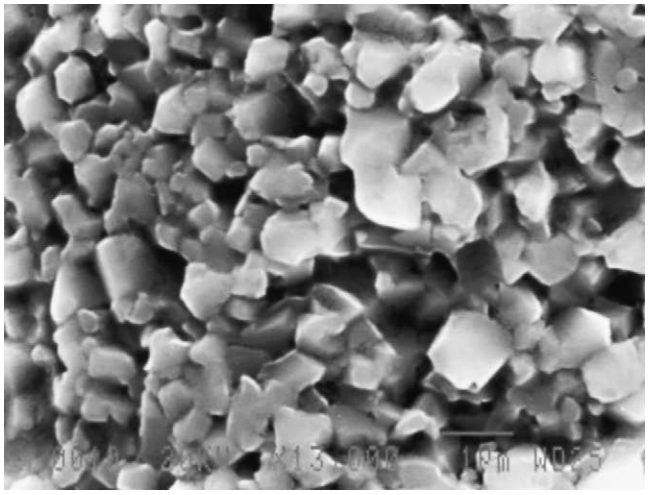

Fig. 10. SEM micrograph of $Li_{1-x}Ni_{1+x}O_2$ prepared from the carboxylate precursor calcined at the optimum temperature and time.

optimum temperature and time, the content of Ni^{3+} and mean oxidation state of nickel are 59.67 wt.% and 2.60, respectively. It shows that the powder prepared from the precursor in air at this condition is the best hexagonal ordering. The XRD spectrum for the precursor calcined at the optimum temperature and time is shown in Fig. 9. Only $Li_{1-x}Ni_{1+x}O_2$ was detected. The peaks are very sharp showing that the powder is good crystalline in nature.

3.8. External morphology

The external morphology of $Li_{1-x}Ni_{1+x}O_2$ prepared from the precursor calcined at the optimum temperature and time was observed using SEM as shown in Fig. 10. The powder consists of 0.3–1.5 μm facet grains, which show good crystallinity. They are in accordance with the XRD results.

4. Conclusions

$Li_{1-x}Ni_{1+x}O_2$ powder was successfully prepared by using malonic acid as a chelating agent and further calcination at 650–800 °C for 14–48 h in air. Due to the TGA results, it is likely that malonic acid can play the role on the decomposition of the acetate ions. The FTIR spectrum of the precursor without calcination shows asymmetric and symmetric COO stretching bands at 1540–1620 and 1360–1450 cm^{-1}, respectively. But for the precursor with 650–800 °C calcination, peaks of metal–oxygen were clearly detected near 550 cm^{-1}. The XRD spectra show a single phase of $Li_{1-x}Ni_{1+x}O_2$(s) at 750 and 800 °C calcination. The minimum $[I_{(006+102)}/I_{(101)}]$ intensity ratio of the XRD spectra, the maximum content of Ni^{3+} and the mean oxidation state of nickel occur at the same calcination temperature of 750 °C. The optimum temperature and time of calcination are at 750 °C and 44 h. Additionally, a possible formation mechanism of $Li_{1-x}Ni_{1+x}O_2$(s) was proposed.

References

[1] Y.S. Lee, Y.K. Sun, K.S. Nahm, Solid State Ionics 118 (1999) 159.
[2] B.J. Hwang, R. Santhanam, C.H. Chen, J. Power Sources 5059 (2002) 1.
[3] Z. Liu, A. Yu, J.Y. Lee, J. Power Sources 81–82 (1999) 416.
[4] C. Delmas, Mater. Sci. Eng. B3 (1989) 97.
[5] S.H. Park, K.S. Park, Y.K. Sun, K.S. Nahm, Y.S. Lee, M. Yoshio, Electrochim. Acta 46 (2001) 1215.
[6] M. Broussely, P. Biensan, B. Simon, Electrochim. Acta 45 (1999) 3.
[7] K. Dokko, M. Nishizawa, S. Horikoshi, T. Itoh, M. Mohamed, I. Uchida, Electrochem. Solid State Lett. 3 (1999) 3.
[8] G.G. Amattucci, J.M. Tarascon, L.C. Klein, J. Electrochem. Soc. 143 (1996) 1114.
[9] C. Delmas, I. Saadoune, Solid State Ionics 53–56 (1992) 370.
[10] E. Zhecheva, R. Stoyanova, Solid State Ionics 66 (1993) 143.
[11] I. Saadoune, C. Delmas, J. Mater. Chem. 6 (1996) 193.
[12] A. Alcantara, J. Morales, J.L. Tirado, R. Stoyanova, E. Zhecheva, J. Electrochem. Soc. 142 (1995) 3997.
[13] J.N. Reimers, J.R. Dalin, J. Electrochem. Soc. 139 (1992) 2091.
[14] C. Delmas, I. Saadoune, A. Rougier, J. Power Sources 43–44 (1993) 595.
[15] S.P. Lin, K.Z. Fung, Y.M. Hon, M.H. Hon, J. Crystal Growth 226 (2001) 148.
[16] M.Y. Song, Ry. Lee, J. Power Sources 111 (2002) 97.
[17] T. Tsumura, S. Kishi, H. Konno, A. Shimizu, M. Inagaki, Thermochim. Acta 278 (1996) 135.
[18] Y.K. Sun, Solid State Ionics 100 (1997) 115.
[19] I.H. Oh, S.A. Hong, Y.K. Sun, J. Mater. Sci. 32 (1997) 3177.
[20] B. Smith, Infrar. Spectr. Interpret., CRC Press, New York, 1999.
[21] W. Li, J.N. Reimers, J.R. Dahn, Phys. Rev. B 46 (1992) 3236.
[22] M.M. Rao, C. Liebenow, M. Jayalakshmi, H. Wulff, U. Guth, F. Scholz, J. Solid State Electrochem. 5 (2001) 348.
[23] M.R. Palacin, D. Larcher, A. Audemer, N. Sac-Epee, G.G. Amatucci, J.M. Tarascon, J. Electrochem. Soc. 144 (1997) 4226.
[24] JCPDS International Centre for Diffract. Data, PA 19073–3273, USA, 2001.
[25] Y.M. Choi, S.I. Pyun, S.I. Moon, Y.E. Hyung, J. Power Sources 72 (1998) 83.
[26] G.T.K. Fey, V. Subramanian, J.G. Chen, Electrochem. Commun. 3 (2001) 234.
[27] D.R. Gaskell, Intro. Metal Therm., second ed., McGraw-Hill Book Co., New York, 1981.
[28] V. Bianchi, D. Caurant, N. Baffier, C. Belhomme, E. Chappel, G. Chouteau, S. Bach, J.P. Pereira-Ramos, A. Sulpice, P. Wilmann, Solid State Ionics 140 (2001) 1.
[29] R. Alcantara, P. Lavela, J.L. Tirado, E. Zhecheva, R. Stoyanova, J. Solid State Electrochem. 3 (1999) 121.
[30] S.P. Lin, K.Z. Fung, Y.M. Hon, M.H. Hon, J. Crystal Growth 234 (2002) 176.
[31] D.F. Shriver, P.W. Atkins, Inorg. Chem., third ed., Oxford University Press, Oxford, 1999.